THE EUROPEAN
PHYSICAL JOURNAL C

Spontaneous scalarization of dyonic black hole in Einstein–Maxwell-scalar theory

Jie Jiang[2,a], **Jia Tan**[1,b]

[1] Jiangsu Key Laboratory of Micro and Nano Heat Fluid Flow Technology and Energy Application, School of Physical Science and Technology, Suzhou University of Science and Technology, Suzhou 215009, China
[2] College of Education for the Future, Beijing Normal University, Zhuhai 519087, China

Abstract In this paper, we study the scalarization of the static and spherically symmetric dyonic Reissner–Nordstrom (RN) black holes in the Einstein–Maxwell-scalar theory where the scalar field is coupled to an electromagnetic Chern–Simons term. When both electric and magnetic charges are present, there exists an unstable region of parametric space for the dyonic RN black holes where the scalarization of black holes should occur. That is to say, mixing electric and magnetic charges can reduce the scalarization in this theory. Firstly, we calculate the perturbation field equations under the dyonic RN black hole background and obtain the corresponding asymptotic-flat perturbation solutions, which are the bifurcation points at the dyonic RN branch. The results show that the perturbation scalarization demands a lower bound of the coupling constant. Then, we calculate the scalarized black hole solutions bifurcating from the dyonic RN solutions. We find that there exist a lot of discrete branches of the scalarized solutions. Contract to the dyonic RN solutions, these scalarized solutions can be overcharged and their mass could even approach zero. After illustrating the behavior of the entropy for the scalarized black holes, we demonstrate that the scalarized configurations might be thermodynamically more stable than GR configurations. Moreover, we also show that for each scalarized branch, the black hole cannot reach the extremal limit with vanishing temperature.

1 Introduction

The no-hair theorem is very important for understanding the properties of black holes. It states that a black hole is uniquely

determined only by three parameters: mass, electric charge, and angular momentum [1–3]. Although the no-hair theory has been proven in Einstein–Maxwell theory, various counterexamples can be found when the gravitational theory possesses an extra field degree of freedom, such as Einstein–Yang–Mills theory [4–6], Dilatonic black holes [7], and a black hole with Skyrme hairs [8–10]. These hairy black hole solutions prompt people to further study the no-hair theorem. The recent developments in the gravitational wave detection [11] and black hole shadow [12] provide us a chance to detect the features of the black hole and then test alternative theories. A key difference between General Relativity (GR) and the alternative theory of gravity is the phenomena of scalarization (a counterexample of the no-hair theorem).

The phenomena of spontaneous scalarization were first investigated for neutron stars in the scalar-tensor theory where the scalar field non-minimally couples to the Ricci curvature [13]. It was illustrated that there is a certain region in parametric space where the scalar-free and scalarized solutions coexist and the scalarized one is energetically favored. After that, the spontaneous scalarization in scalar-tensor theories was extended to the black hole cases [14,15]. Recently, the spontaneous scalarization was widely studied in extended scalar-tensor-Gauss-Bonnet gravity, in which the scalar field is non-minimally coupled to a Gauss-Bonnet gravity correction term [16–27]. The dynamics of spontaneous black hole scalarization in Einstein-Scalar-Gauss–Bonnet gravity is also investigated in Ref. [28–30]. Moreover, this mechanism is also studied in Einstein–Chern–Simons-Scalar theory with a scalar field non-minimally coupled to a Chern–Simons gravity correction term [31–35]. In these models, spontaneous scalarization is induced by the geometry of spacetime. Alternatively, this mechanism can also be found in the Einstein–Maxwell-scalar models where the scalar field is non-minimally coupled to some Maxwell invariant terms.

[a] e-mail: jiejiang@mail.bnu.edu.cn

[b] e-mail: jiatansust@163.com (corresponding author)

Springer

The non-minimally coupled part of Lagrangian density can be generally expressed as

$$\mathscr{L}_{\text{int}} = \mathscr{F}(\phi) I(F_{ab}), \tag{1}$$

in which ϕ is the scalar field, F_{ab} is the electromagnetic strength, and $\mathscr{F}(\phi)$ is a coupling function. In Ref. [36], the scalarization of a charged black holes in Einstein–Maxwell-scalar models with an exponential coupling function and a Maxwell invariant term $I = F_{ab}F^{ab}$ are taken into consideration, in which the fully non-linear evolution of spontaneous scalarization of a spherically symmetric black hole is also presented. Later, spontaneous scalarization in Einstein–Maxwell-scalar theories was extended to various situations, such as the cases with other coupling functions [37–39], reflecting stars without horizon [40], Einstein–Born–Infeld-scalar theory [41], Einstein–Maxwell-scalar theory with a quasitopological term [42], higher-dimensional scenario [43], dyonic black hole with magnetic charges [44], and non-asymptotically flat black holes [45–48]. Furthermore, the linear stability and quasinormal modes of scalarized black holes [49–53], analytic treatments of spontaneous scalarization [54–56], and dynamical scalarization [57–61] were also widely discussed in Einstein–Maxwell-scalar theories.

For the Einstein–Maxwell-scalar theories mentioned above, the Maxwell invariant term is chosen as $F_{ab}F^{ab}$, $F_a^b F_b^c F_c^a$ or their function. Apart from these Maxwell invariant quantities, the electromagnetic Chern–Simons term $I_{\text{CS}} = \epsilon_{abcd} F^{ab} F^{cd}$ is also a candidate as a Maxwell invariant coupled to the scalar (pseudoscalar) field and this term will violate the parity invariance. Usually the pseudoscalar field is also called axion and it is widely applied in the cosmology and astronomy to study the dark matter [62–67]. When the coupling function is a constant, this term is just a pure topological term and does not contribute to the equation of motion. Moreover, different from $F_{ab}F^{ab}$, the electromagnetic Chern–Simons term is nonvanishing only for the case where both electric and magnetic charges are present. For nonvanishing electric and magnetic charges, I_{CS} shows a similar feature as $F_{ab}F^{ab}$. Moreover, there are a lot of similarities between this theory and the geometric Einstein–Chern–Simons-Scalar theory, which can also induce the spontaneous scalarization and violates the parity invariance. That is to say, this flavor of Einstein–Maxwell-scalar theory can help us build intuition about the scalarization in Chern–Simons gravity in a much easier way because of its relatively simple field equations. Then, it is natural to ask whether spontaneous scalarization can occur in this model. Therefore, in this paper, we would like to consider the dyonic Reissner–Nordstrom (RN) black holes in the Einstein–Maxwell-scalar theory where the scalar field is coupled to an electromagnetic Chern–Simons term and investigate whether the mixing of electric and magnetic charges can reduce the spontaneous scalarization.

The outline of this paper is as follows. In Sect. 2, we briefly introduce the Einstein–Maxwell-scalar theory in which the scalar field couples to an electromagnetic Chern–Simons term and obtain the equations of motion in the static and spherically symmetric configurations. In Sect. 3, we study the stability of the dyonic RN black hole under the perturbations and evaluate the perturbation scalar field satisfied the asymptotic flatness condition, i.e., the bifurcation points of the dyonic RN solution and scalarized black hole solution. In Sect. 4, based on the shooting method, we calculate the scalarized dyonic RN black hole solutions numerically and discuss their properties. Finally, the conclusion and discussion are presented in Sect. 5.

2 Einstein–Maxwell-scalar model with an electromagnetic Chern–Simons term

In this paper, we would like to consider the Einstein–Maxwell-scalar theory where the scalar or pseudoscalar field is coupled to an electromagnetic Chern–Simons term. Noting that the Chern–Simons term violates the parity invariance, i.e., it is a pseudoscalar, then the coupling function $\mathscr{F}(\varphi)$ should also be a pseudoscalar to ensure the theory is parity invariant. With this in mind, most of the literature only considers the linear coupling between the pseudoscalar field and the electromagnetic Chern–Simons term [62–67]. Motivated by the phenomenon of spontaneous scalarization widely discussed in the quadratic Einstein-scalar-Gauss–Bonnet gravity [49–53], we want to consider the quadratic coupling function such that the theory admits both the dyonic Reissner–Nordstrom black hole and scalarized black hole solutions. In order to ensure that the theory is parity invariant and also has a quadratic coupling function, we introduce a scalar and a pseudoscalar field into the theory, in which the action is given by

$$S = \frac{1}{16\pi} \int d^4 x \sqrt{g} \Big[R - 2\nabla_a \varphi_1 \nabla^a \varphi_1 - 2\nabla_a \varphi_2 \nabla^a \varphi_2$$
$$- F_{ab}F^{ab} + \mathscr{F}(\varphi_1, \varphi_2) I_{\text{CS}} \Big] \tag{2}$$

with the coupling function

$$\mathscr{F} = \frac{\lambda^2}{2} \varphi_1 \varphi_2 \tag{3}$$

and the Chern–Simons term of the electromagnetic field

$$I_{\text{CS}} = \epsilon_{abcd} F^{ab} F^{cd}, \tag{4}$$

where λ is a conpling constant, R is the Ricci scalar of the spacetime metric g_{ab}, φ_1 is a scalar field, φ_2 is a pseudoscalar field, $F_{ab} = \nabla_a A_b - \nabla_b A_a$ with the vector potential A_a is the electromagnetic strength. In this theory, the parity invariance

is restored duce to the pseudoscalar field. For convenience, we define

$$\varphi = \frac{1}{\sqrt{2}}(\varphi_1 + \varphi_2), \quad \bar{\varphi} = \frac{1}{\sqrt{2}}(\varphi_1 - \varphi_2). \qquad (5)$$

Then, the coupling function becomes

$$\mathscr{F} = \frac{\lambda^2}{2}(\varphi^2 - \bar{\varphi}^2). \qquad (6)$$

By variation of the action, the equations of motion can be obtained and it is given by

$$R_{ab} - \frac{1}{2}Rg_{ab} = 2\nabla_a\varphi\nabla_b\varphi - g_{ab}\nabla_c\varphi\nabla^c\varphi + 2\nabla_a\bar{\varphi}\nabla_b\bar{\varphi}$$
$$-g_{ab}\nabla_c\bar{\varphi}\nabla^c\bar{\varphi} + 2F_{ac}F^c{}_b$$
$$-\frac{1}{2}g_{ab}F_{cd}F^{cd},$$
$$\nabla_a F^{ab} = -\epsilon^{abcd}F_{cd}\nabla_a\mathscr{F},$$
$$\nabla_a\nabla^a\varphi = -\frac{\lambda^2}{4}I_{\text{CS}}\varphi,$$
$$\nabla_a\nabla^a\bar{\varphi} = \frac{\lambda^2}{4}I_{\text{CS}}\bar{\varphi}. \qquad (7)$$

From the equation of motion, we can see that the Chern–Simons term does not affect the gravitational part of the equations of motion, i.e., it does not contribute to the stress-energy tensor of the scalar field and electromagnetic field. However, it can influence the equation of motion of the scalar field, and the Chern–Simons term can be regarded as the effective potential of the scalar field, which makes the scalarization possible in this theory.

In this paper, we focus on the static and spherically symmetric dyonic black hole solution in which the scalar field and electromagnetic field have the same symmetries. We adopt the following ansatz for the line element

$$ds^2 = -f(r)dv^2 + 2\alpha(r)dvdr + r^2(d\theta^2 + \sin^2\theta d\phi^2). \qquad (8)$$

For the dyonic solution, considering the symmetries of the electromagnetic field and together with the Maxwell equation in Eq. (7), the electromagnetic strength is obtained and it is given by

$$\mathbf{F} = -\frac{Q_e\alpha(r)}{r^2}\left(1 + \frac{2Q_m\mathscr{F}}{Q_e}\right)dt \wedge dr$$
$$+ Q_m\sin\theta d\theta \wedge d\phi, \qquad (9)$$

where

$$Q_e \equiv \frac{1}{4\pi}\int_\infty [\star\mathbf{F} - 2\mathscr{F}\mathbf{F}], \quad Q_m \equiv \frac{1}{4\pi}\int_\infty \mathbf{F} \qquad (10)$$

are the electric charge and magnetic charge, separately. Using the above results, the Chern–Simons term becomes

$$I_{\text{CS}} = \frac{8Q_m}{r^4}[Q_e + 2Q_m\mathscr{F}], \qquad (11)$$

which means the purely electric solution will reduce to the Einstein–Maxwell-scalar theory without the Chern–Simons corrections and the no-hear theorem will be valid. Therefore, we only consider the dyonic solution with the magnetic charge in this paper. From the field equations for the scalar fields, we can see that the signs of the effective potential for φ and $\bar{\varphi}$ are opposite. That is to say, one of them has to be stable under the dyonic Reissner–Nordstrom black hole background, and only one scalar field can lead to spontaneous quantization. In this paper, we only consider the scalarized solution induced by φ and set $\bar{\varphi} = 0$ (The opposite case can be obtained by changing the sign of Q_eQ_m). Then, using the line element (8), the equations of motion reduce to

$$r^3\alpha f' + r^2(\alpha - 2r\alpha' + r^2\alpha\varphi'^2)f$$
$$+[Q_e^2 + Q_m^2 + 4Q_eQ_m\mathscr{F}(\varphi)$$
$$+4Q_m^2\mathscr{F}(\varphi)^2 - r^2]\alpha^3 = 0,$$
$$2\alpha^3 - 2f\left(2r^2\alpha\varphi'^2 - 3r\alpha' + \alpha\right)r^2f'\alpha'$$
$$+r^2f'\alpha' - r\alpha\left(rf'' + 4f'\right) = 0,$$
$$r^3\alpha\left[rf'\varphi' + f\left(r\varphi'' + 2\varphi'\right)\right] - r^4f\alpha'\varphi'$$
$$+2Q_m\alpha^3\mathscr{F}'(\varphi)[Q_e + 2Q_m\mathscr{F}(\varphi)] = 0. \qquad (12)$$

When the scalar field is vanishing, i.e., $\varphi = 0$, this theory admits the dyonic Reissner–Nordstrom black hole solution in which

$$f(r) = 1 - \frac{2M}{r} + \frac{Q_e^2 + Q_m^2}{r^2}, \qquad \alpha(r) = 1,$$
$$\mathbf{F} = -\frac{Q_e}{r^2}dt \wedge dr + Q_m\sin\theta d\theta \wedge d\phi, \qquad (13)$$

in which M is the mass of the black hole. The event horizon exists if $M^2 \geq Q_e^2 + Q_m^2$ and the radius of horizon is given by $r = r_h$ with

$$r_h = M + \sqrt{M^2 - Q_e^2 - Q_m^2}. \qquad (14)$$

3 Stability and perturbation of dyonic Reissner–Nordstrom black hole

The scalarized black hole solution may appear in the regions of the parameteric space in which the corresponding solution becomes unstable. Next, we consider the perturbations of the scalar field, electromagnetic field, and metric for the dyonic Reissner–Nordstrom black hole. From the equations of motion (7), it is not hard to see that the scalar field perturbation $\delta\varphi$ is decoupled to the perturbations δg_{ab} and δA_a of the metric and electromagnetic field, which means that the stability is only determined by the scalar field perturbation. The perturbation equation of the scalar field is given by

$$\nabla_a\nabla^a\delta\varphi + \frac{\lambda^2}{4}I_{\text{CS}}\delta\varphi = 0, \qquad (15)$$

in which the covariant derivative ∇_a and the Chern–Simons term I_{CS} are evaluated in the dyonic Reissner–Nordstrom geometry (13). Since the background geometry considered is a static and spherically symmetric black hole, we can perform a spherical harmonics decomposition of the scalar field

$$\delta\varphi = \frac{u(r)}{r} Y_{lm}(\theta, \phi)e^{-i\omega t}, \qquad (16)$$

in which $t \equiv v - r^*$ with the tortoise coordinate $r_*(r) = \int f(r)^{-1} dr$, and ω is the frequency of the quasinormal modes (QNM). Then, the perturbation equation becomes

$$\frac{d^2u}{dr_*^2} + [\omega^2 - U(r)]u = 0 \qquad (17)$$

with the effective potential

$$U(r) = f(r) \left(\frac{l(l+1)}{r^2} + \frac{2M}{r^3} - \frac{2Q_{tot}^2}{r^4} - \frac{2\lambda^2 Q_e Q_m}{r^4} \right), \qquad (18)$$

in which Q_{tot} denotes the total charge defined by

$$Q_{tot}^2 = Q_e^2 + Q_m^2. \qquad (19)$$

With some physical limitations [69], we require that there is only the ingoing wave near the event horizon and only the outgoing wave at asymptotic infinity, i.e.,

$$\delta\varphi \sim e^{-i\omega r_*}, \quad r \to r_+,$$
$$\delta\varphi \sim e^{i\omega r_*}, \quad r \to \infty. \qquad (20)$$

From the above setups, the unstable QNM frequencies should have negative imaginary part, which means that the boundary conditions for the unstable modes are vanishing at the event horizon and asymptotic infinity.

It has been showed in Ref. [68] that if the potential satisfies the condition

$$\int_{r_H}^{\infty} \frac{U(r)}{f(r)} dr < 0, \qquad (21)$$

there will exist an unstable mode for the perturbation scalar field. Since we only consider the spherically symmetric solution, we set $l = 0$. As mentioned above, the scalarization can only appear for the case with a nonvanishing magnetic charge, also with the nonvanishing total charge. Therefore, in the following, we normalize the electric, magnetic charges and mass to the total charge Q_{tot}, i.e., $\tilde{Q}_e = Q_e/Q_{tot}$, $\tilde{Q}_m = Q_m/Q_{tot}$ and $\tilde{M} = M/Q_{tot}$. From the perturbation field equation (15), we can see that the solution is only dependent on the reduced mass $\tilde{M}$ as well as the quantity $\tilde{Q}_e\tilde{Q}_m\lambda^2$. To simplify, we introduce the notation

$$\zeta = 2\tilde{Q}_e\tilde{Q}_m\lambda^2. \qquad (22)$$

Using the identity $Q_{tot}^2 = Q_e^2 + Q_m^2 \geq 2Q_eQ_m$, we have $2\tilde{Q}_e\tilde{Q}_m \leq 1$ and therefore $\lambda^2 \geq \zeta$. With these setups, the unstability condition (21) gives
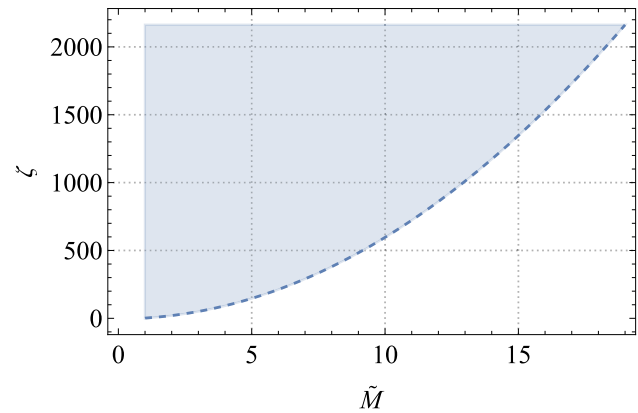

Fig. 1 Unstable regions of the parametric space for the perturbation scalar field based on the condition (21) from integral of the potential

$$\zeta > 3\tilde{M}^2 - 2 + 3\tilde{M}^2\sqrt{\tilde{M}^2 - 1}. \qquad (23)$$

Note that the right-hand side of this inequality is always positive and the minimum value is one. Then, a necessary condition for the validity of the above inequality is

$$\lambda^2 \geq \zeta > 1, \qquad (24)$$

which also gives $\tilde{Q}_e\tilde{Q}_m \geq 0$, i.e., the electric charge and magnetic charge have the same signature. Without loss of generality, we set $Q_e > 0$ and $Q_m > 0$. If the inequality (23) is satisfied, the dyonic Reissner–Nordstrom black hole will become unstable. In Fig. 1, we showed the unstable regions of the parametric space. This figure shows that as $\tilde{Q}_e\tilde{Q}_m$ or λ becomes larger and larger, the perturbation scalar field becomes more and more unstable. The coupling parameter λ presents the interaction strength between the scalar field and the electromagnetic field, and the quantity $\tilde{Q}_e\tilde{Q}_m$ gives how large the Chern–Simons term is. It means that stronger interaction from the electromagnetic field can destabilize the perturbation scalar field.

Next, we would like to solve the static and spherically symmetric solution of the perturbation equation (15) by demanding that the scalar field is regular on the horizon and vanishing at infinity, which comes from the requirement for asymptotic flatness at infinity. These perturbation solutions are the bifurcation points of dyonic RN solution and scalarized black hole solution, which also represents the onset of scalarization and instability. It is worth mentioning that this boundary condition is not inconsistent with the boundary condition (20) for the unstable mode since the QNMs considered here are the onset of the instability and their frequencies should have vanishing negative imaginary parts.

For the static and spherical scalar field, the field equation (15) becomes

$$f\delta\varphi'' + \left(f' + \frac{2f}{r} \right)\delta\varphi' + \frac{2\lambda^2 Q_e Q_m}{r^4}\delta\varphi = 0, \qquad (25)$$
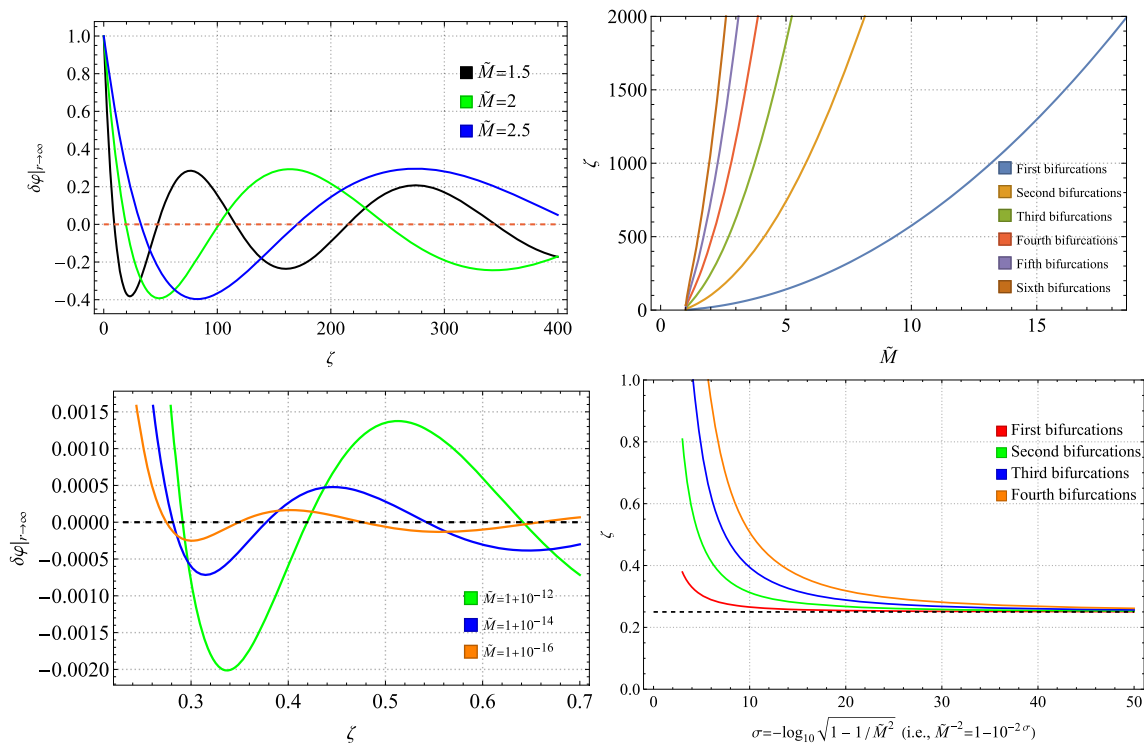
Fig. 2 The left two panels show the asymptotic value $\delta\varphi|_{r\to\infty}$ of the perturbation scalar field as a function of the parameter $\zeta = 2\tilde{Q}_e\tilde{Q}_m\lambda^2$ for different reduced mass $\tilde{M} = M/Q_{\mathrm{tot}}$. The top right panel shows the parameters $(\zeta, \tilde{M})$ of the first six bifurcations (the perturbation solutions of the scalar field satisfying the asymptotic flatness condition) from the dyonic RN black hole, and the bottom right panel shows its behavior near the extremal black holes (i.e., $\tilde{M} \gtrsim 1$)

in which $\delta\varphi$ is only a function of r and $f(r)$ is the blackening factor given by Eq. (13). For this field equation, one can find an exact solution

$$\delta\varphi(r) = c_1 P_y(x) + c_2 Q_y(x), \tag{26}$$

where

$$y = -\frac{1 + \sqrt{1 - 4\zeta}}{2}, \quad x = \frac{1 - \tilde{M}\tilde{r}}{\tilde{r}\sqrt{\tilde{M}^2 - 1}}. \tag{27}$$

Here $\tilde{r} = r/Q_{\mathrm{tot}}$ is the reduced radius coordinate, $P_y(x)$ and $Q_y(x)$ are the Legendre function of the first and second kinds separately. Considering the regularity of the scalar field on the horizon, i.e., the perturbation scalar field is finite at $r = r_h$, we can fix the undetermined coefficients and the solution is given by

$$\delta\varphi(r) \propto \cos(\pi y)P_y(x) - \frac{2\sin(\pi y)}{\pi}Q_y(x), \tag{28}$$

in which we can simply set $\delta\varphi(r_h) = 1$ since the field equation is linear. Then, getting the bifurcation points from a dyonic RN black hole is equivalent to finding the appropriate parameters such that its linear solution satisfies the asymptotic flatness condition $\delta\varphi|_{r\to\infty} = 0$. That is to say, $\delta\varphi|_{r\to\infty}$ should be regarded as a function of the parametric space and we need to study the zeros of this function. In

the top left panel of Fig. 2, we show the asymptotic value $\delta\varphi|_{r\to\infty}$ of the perturbation scalar field as a function of ζ for $\tilde{M} = 1.5$, $\tilde{M} = 2$ and $\tilde{M} = 2.5$. This figure shows that there exist some discrete parameters ζ such that their corresponding solutions satisfy the asymptotic flatness condition. These parameters are the bifurcation points of the dyonic RN solution and scalarized black hole solution. We show the first six bifurcations in the top right panel of Fig. 2. There are more bifurcations that we have not shown in the figure and they are located on the left side near the extremal parameters $\tilde{M} = 1$. This figure also shows that for a given ζ, the first bifurcations give the largest reduced mass $\tilde{M}$. In the bottom two panels of Fig. 2, we illustrate the behaviors near the extremal black holes (i.e., $\tilde{M} \gtrsim 1$). From these figures, one can note that as $\tilde{M} \to 1$, each bifurcation gets closer and closer to each other and eventually approaches 1/4. That is to say, the existence of the bifurcation requires ζ above a minimal value 1/4, i.e., $\zeta \geq 1/4$, which also implies that $\lambda^2 \geq 1/4$. This shows a lower bound than the previous one (24) from the stability analysis, which is also showed. However, it is reasonable since the performed stability analysis provides only a sufficient condition for instability and does not mean that the scalarization cannot occur outside this condition, see Fig. 3, which also implies that the actual unstable region should be larger than that given by Eq. (21).
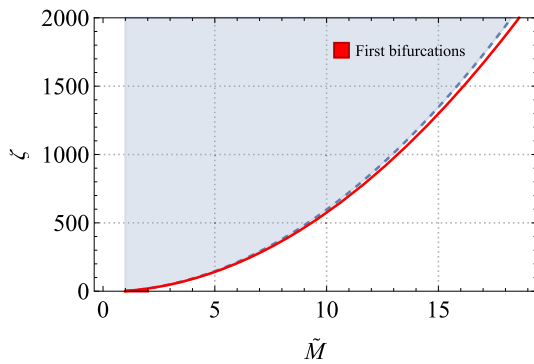
Fig. 3 The red line shows the first bifurcations of the scalar field and the shaded region presents the unstable regions based on the condition (21) from integral of the potential

4 Scalarization of dyonic RN black hole

In this section, we would like to evaluate the scalarized black hole solutions bifurcating from the dyonic RN solution of the field equations (12) using a shooting method. These black hole solutions are required to be regular on the black hole horizon and satisfy the asymptotic flatness condition. Asymptotic flatness condition demands

$$f|_{r\to\infty} = \alpha_\infty^2, \quad \text{and} \quad \varphi|_{r\to\infty} = 0. \tag{29}$$

with $\alpha_\infty = \alpha|_{r\to\infty}$. This condition implies that the asymptotic line element can be expressed as

$$ds^2|_{r\to\infty} \simeq -du^2 + 2du\,dr + r^2(d\theta^2 + \sin^2\theta\,d\phi^2) \tag{30}$$

with $u = \alpha_\infty v$, which describes a flat geometry at infinity. Then, we can expand these functions to infinity, i.e.,

$$f(r) = \alpha_\infty^2 - \frac{2M\alpha_\infty^2}{r} + \mathcal{O}(1/r^2),$$
$$\varphi(r) = \frac{D}{r} + \mathcal{O}(1/r^2) \tag{31}$$

at $r \to \infty$. Here M and D are the mass of the black hole and the charge of the scalar field individually. Considering the regularity condition and together with $f(r_h) = 0$, we can expand the metric function and scalar field at $r = r_h$,

$$f(r) = (r - r_h)f'(r_h) + \mathcal{O}((r - r_h)^2),$$
$$\alpha(r) = \alpha_h + (r - r_h)\alpha'(r_h) + \mathcal{O}((r - r_h)^2),$$
$$\varphi(r) = \varphi_h + (r - r_h)\varphi'(r_h) + \mathcal{O}((r - r_h)^2), \tag{32}$$

in which we denote $\varphi_h = \varphi(r_h)$ and $\alpha_h = \alpha(r_h)$. Using the equation of motion (12), we can further obtain

$$f'(r_h) = -\frac{\alpha_h^2(Q_{\text{tot}}^2 - r_h^2 + 2\lambda^2 Q_m Q_e \varphi_h^2 + \lambda^4 Q_m^2 \varphi_h^4)}{r_h^3},$$

$$\varphi'(r_h) = \frac{2\varphi_h(\lambda^2 Q_e Q_m + \lambda^4 Q_m^2 \varphi_h^4)}{r_h(Q_{\text{tot}}^2 - r_h^2 + 2\lambda^2 Q_m Q_e \varphi_h^2 + \lambda^4 Q_m^2 \varphi_h^4)},$$

$$\alpha'(r_h) = -\frac{4\alpha_h \varphi_h^2(\lambda^2 Q_e Q_m + \lambda^4 Q_m^2 \varphi_h^4)^2}{3r_h(Q_{\text{tot}}^2 - r_h^2 + 2\lambda^2 Q_m Q_e \varphi_h^2 + \lambda^4 Q_m^2 \varphi_h^4)^2}. \tag{33}$$

For a black hole solution, we need $f'(r_h) \geq 0$, which leads to

$$\varphi_h^2 \leq \frac{r_h^2 - Q_{\text{tot}}^2}{\lambda^2 Q_m \left(\sqrt{r_h^2 - Q_m^2} + Q_e\right)}. \tag{34}$$

The existence of a scalarized black hole solution demands that the right-hand side of the above inequality is positive, i.e.,

$$r_h \geq |Q_{\text{tot}}|. \tag{35}$$

Without loss of generality, we can set $\alpha_h = 1$ by changing the coordinate $v \to v/\alpha(r_h)$. For the fixed coupling constant λ, electric charge Q_e and magnetic charge Q_m, the above discussion implies that all the series coefficients for the function $f(r)$, $\varphi(r)$ and $\varphi(r)$ can be calculated in terms of φ_h and r_h. Then, we can use the series expansions to evaluate values of the functions near the event horizon and perform them as initial values to solve the field equations. Same to the perturbation cases, getting the scalarized dyonic RN black hole reduces to finding the appropriate initial values φ_h and r_h such that its solution satisfies the asymptotic flatness conditions (29). From the field equations (12), we can see that the first condition of Eq. (29) is automatically satisfied at infinity. Therefore, we only need to find the initial parameters which meet the condition $\varphi|_\infty = \varphi|_{r\to\infty} = 0$. In Fig. 4, we illustrate the asymptotic value φ_∞ of the scalar field as a function of horizon radius r_h for fixed $\lambda = 3$, $\tilde{Q}_m = 0.5$ and for fixed $\lambda = 6$, $\tilde{Q}_m = 0.5$ with different values $\varphi_h = 0.03, 0.06, 0.09$. These figures show that there exist some discrete zero-points of φ_∞ which give the scalarized dyonic RN solutions and these discrete solutions can give the discrete branches of scalarized solution. Then, we present the metric functions $f(r)$, $\alpha(r)$ and scalar field $\varphi(r)$ as a function of r/r_h with some fixed λ, $\tilde{Q}_m$ and φ_h for the first three solutions of dyonic RN black holes in Fig. 5, where we rank these solutions by the distance between their horizon radius and the extremal radius

$$r_h^{\text{ext}} = \sqrt{Q_{\text{tot}}^2 + 2\lambda^2 Q_m Q_e \varphi_h^2 + \lambda^4 Q_m^2 \varphi_h^4}, \tag{36}$$

which leads to $f'(r_h^{\text{ext}}) = 0$. From these figures, we can note that there does not exist a zero-point for the scalar field
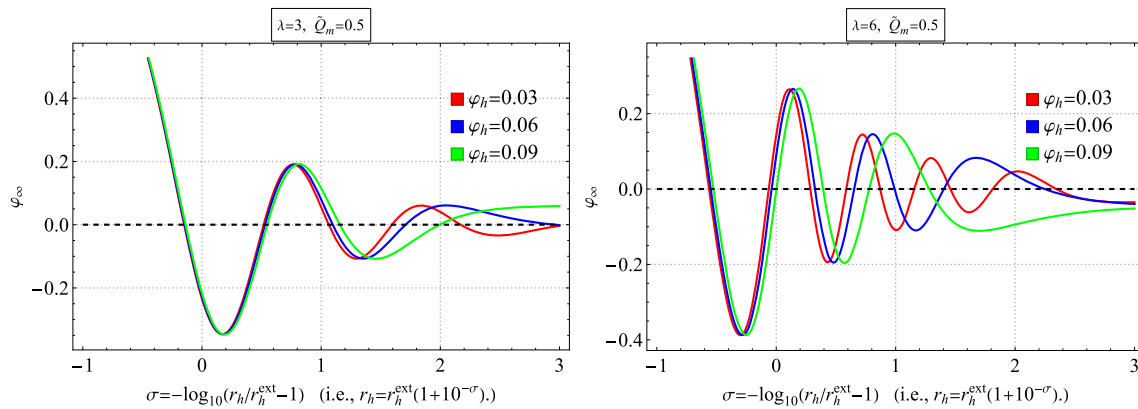
Fig. 4 Plots show the asymptotic value φ_∞ of the scalar field as a function of horizon radius r_h for fixed coupling constant λ, reduced magnetic charge $\tilde{Q}_m$ and horizon-value φ_h of the scalar field. Here we denote the extremal horizon radius $r_h^{\text{ext}} = \sqrt{Q_{\text{tot}}^2 + 2\lambda^2 Q_m Q_e \varphi_h^2 + \lambda^4 Q_m^2 \varphi_h^4}$ and we have $r_h \geq r_h^{\text{ext}}$
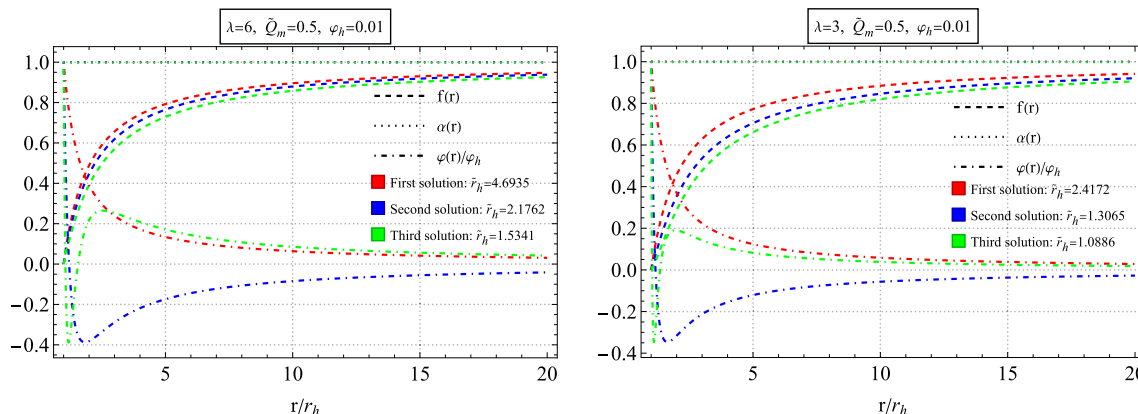

Fig. 5 Plots show the behaviors of metric functions and scalar field as a function of r/r_h with the fixed λ, $\tilde{Q}_m$ and φ_h for the first three solutions of scalarized dyonic RN black hole

$\varphi(r)$ of the first solution, while the second and third solutions have one and two zero-points, separately. Similar features can also be captured for the other scalarized solution and these imply that the number of zero-points of $\varphi(r)$ increases as the solution gets closer to the extreme for fixed λ, $\tilde{Q}_m$ and φ_h.

After giving λ and $\tilde{Q}_m$, a fixed φ_h can determine the discrete scalarized solutions with some r_h. By varying φ_h, we can obtain the discrete branches of scalarized solution in the parametric space (φ_h, r_h). For a given scalarized solution, using Eq. (31), we can obtain its corresponding mass M and scalar charge D. In Fig. 6, we show the behavior of the reduced scalar charge $\tilde{D} = D/Q_{\text{tot}}$ as a function of the reduced black hole mass $\tilde{M}$ with series values of the coupling constant λ and reduced magnetic charge $\tilde{Q}_m$ for the first three branches of scalarized dyonic RN black hole. When $\tilde{D}$ and $\tilde{\varphi}_h$ approach zero, the solutions (bifurcations) can be described by the results from perturbation analysis. In Table 1, we show the difference between the first three bifurcations calculated by solving the nonlinear equations and the per-

turbation equation respectively. As a result, we can see that $R = \tilde{M}_1/\tilde{M}_2 = 1 + \mathcal{O}(\tilde{\varphi}_h)$ for small $\tilde{\varphi}_h$, in which $\tilde{M}_1$ is the reduced mass for small $\tilde{\varphi}_h$ from the nonlinear calculations and $\tilde{M}_2$ is the reduced mass from the perturbation analysis. That is to say, all the branches of the scalarized solution bifurcate with the GR branch of the dyonic RN black hole and the bifurcation points can be determined by the perturbation scalarized solutions given by Sect. 3. For the GR branch, the existence of the black hole demands that $\tilde{M} \geq 1$, i.e., $M^2 \geq Q_{\text{tot}}^2$. However, the reduced mass $\tilde{M}$ of the scalarized branches can be less than one or even approach zero, i.e., the scalarized dyonic black hole can be overcharged. This means that the scalarized dyonic RN solution enlarges the range of mass in GR. One can also note from Fig. 6 that the absolute value of the black hole scalar charge smoothly decreases with the mass and the maximal value is reached when the black hole mass approaches zero. Moreover, these figures also illustrate that the absolute value of scalar charge increases as λ or $Q_e Q_m$ increase when we fixed the black
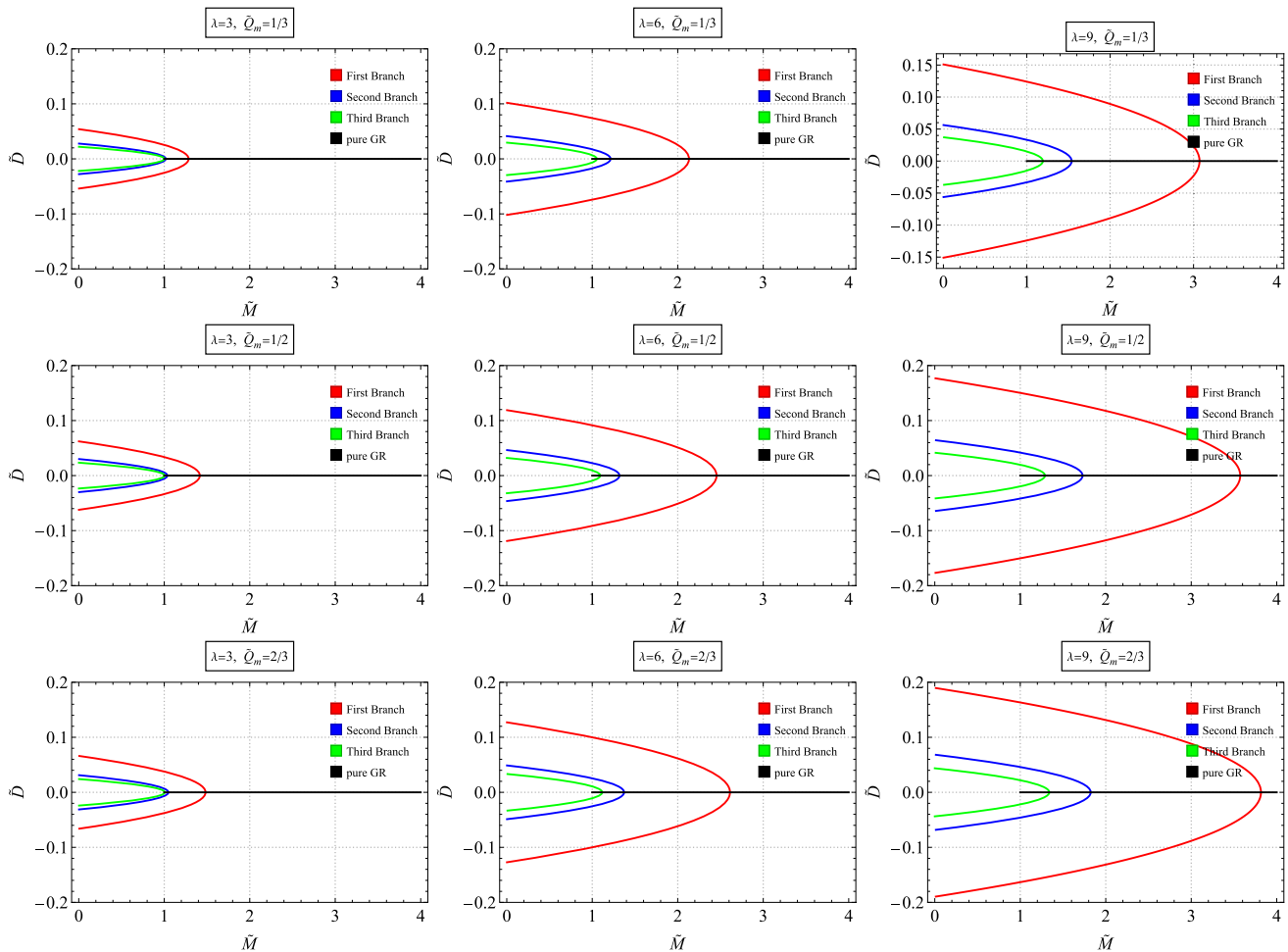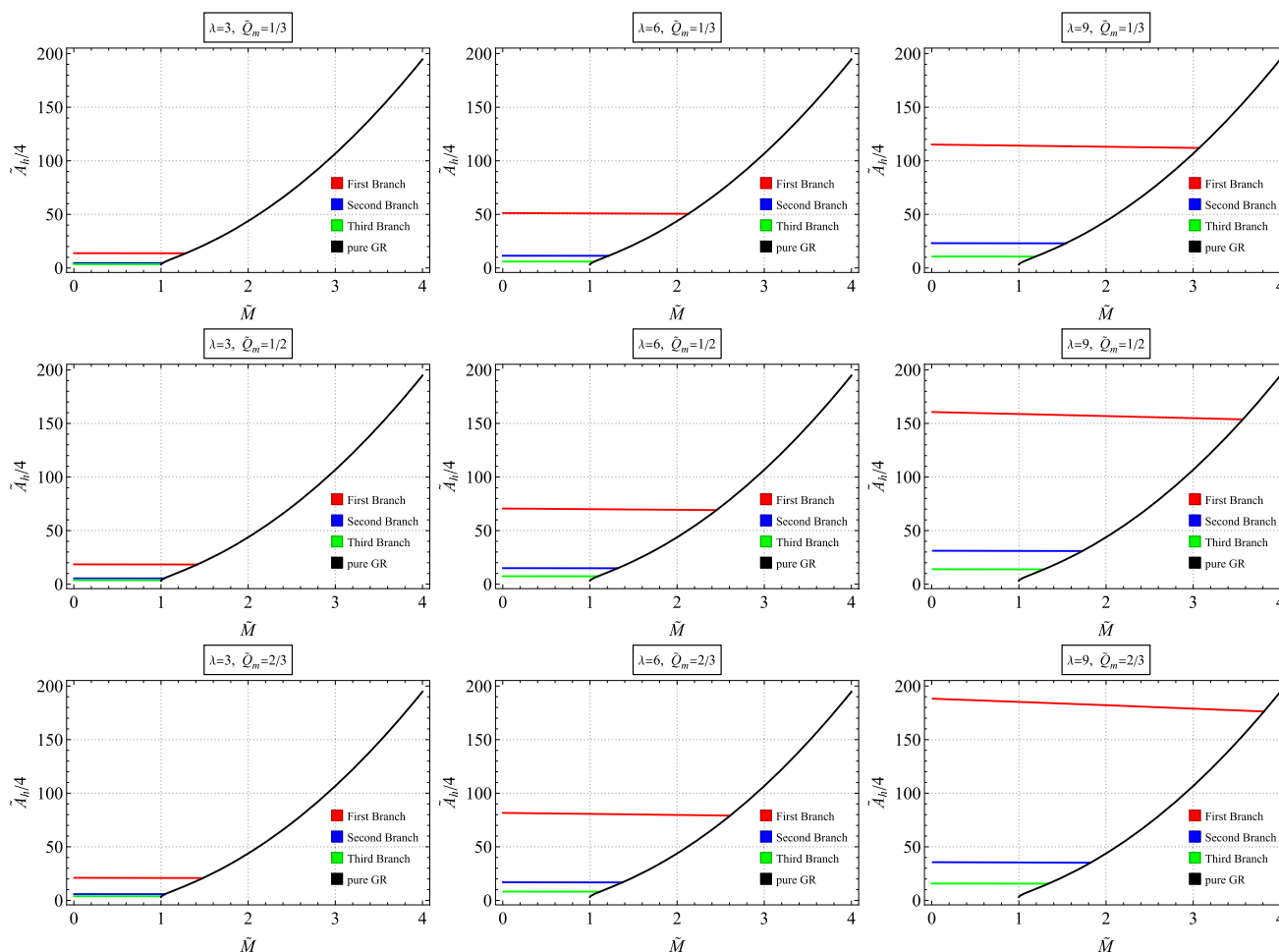
Fig. 6 Plots show the reduced scalar charge $\tilde{D}$ of black holes as a function of its reduced mass $\tilde{M}$ with different values of the coupling constant λ and reduced magnetic charge $\tilde{Q}_m$ for the first three branches of scalarized dyonic RN black hole

hole reduced mass $\tilde{M}$. From Eq. (11), we can see that the larger λ and $Q_e Q_m$ indicate stronger interaction between the electromagnetic field and scalar field. That is to say, the stronger interaction can lead to larger scalar hair and also enlarge the parametric region of the scalarized solution.

With a similar consideration as Ref. [18], to have an indicator for the stability, it is illustrated in Fig. 7 that the behavior of the reduced black hole entropy $\tilde{A}_h/4 = \pi \tilde{r}_h^2$ of the first three scalarized branches as a function of its reduced mass $\tilde{M}$ for some given λ and $\tilde{Q}_m$. We see that all scalarized branches start from a bifurcation point at the GR branch and the entropy for all scalarized solutions exceeds the counterpart of dyonic RN solution with the same reduced mass $\tilde{M}$. This indicates that the scalarized configurations might be thermodynamically more stable compared to the GR configuration. For different scalarized branches, one can see that the entropy of the second and third branches is lower than the first branch, which implies that the first scalarized branch is the most stable one. Moreover, we can also note from Fig. 7 that

the entropy of scalarized solutions increases as λ and $Q_e Q_m$ increase, which means that the stronger interaction can make the scalarized configuration more stable. Together with the result indicated in Fig. 6, these imply that the scalarization might be more likely to appear in situations with stronger interaction between the scalar field and electromagnetic field.

In Fig. 8, we show the behavior of the reduced black hole temperature $\tilde{T} = f'(r_h)/4\pi$ as a function of its reduce mass M with different values of λ and $\tilde{Q}_e$ for the first three scalarized branches and GR branches. These figures show that the scalarized dyonic RN black hole solutions cannot reach the extremal limit $T = 0$ different from the GR branch where the zero-temperature can be obtained for $\tilde{M} = 1$. This is because the scalarized branches are ended at the point where the spacetime mass vanishes. Moreover, from these figures, we can also see that different from the entropy of the scalarized black holes, the maximal temperature is not always given by the first branch and is determined by the relative position of the scalarized branches for the fixed λ and $\tilde{Q}_m$.

Table 1 The table shows the ratio $R = \tilde{M}_1/\tilde{M}_2$ for small $\tilde{\varphi}_h = 10^{-3}$ with different parameters, in which $\tilde{M}_1$ is the reduced mass for small $\tilde{\varphi}_h$ from the nonlinear calculations and $\tilde{M}_2$ is the reduced mass from the perturbation analysis

	$\lambda = 3, \tilde{Q}_m = 1/3$	$\lambda = 6, \tilde{Q}_m = 1/3$	$\lambda = 9, \tilde{Q}_m = 1/3$	$\lambda = 3, \tilde{Q}_m = 2/3$	$\lambda = 6, \tilde{Q}_m = 2/3$	$\lambda = 9, \tilde{Q}_m = 2/3$
First bifurcations	0.999964	0.999961	0.999963	0.999960	0.999965	0.999970
Second bifurcations	0.999985	0.999970	0.999959	0.999979	0.999969	0.999967
Third bifurcations	0.999994	0.999979	0.999976	0.999995	0.999977	0.999981

Fig. 7 Plots show the reduced entropy $\tilde{A}_h/4$ of black holes as a function of its reduced mass $\tilde{M}$ with different values of the coupling constant λ and reduced magnetic charge $\tilde{Q}_m$ for the first three branches of scalarized dyonic RN black hole

5 Conclusion and discussion

In the current paper, we considered the Einstein–Maxwell-scalar theory where the scalar field is coupled to an electromagnetic Chern–Simons term, and studied the scalarization of the static and spherically symmetric dyonic RN black holes in this theory. The Chern–Simons term is nonvanishing only if neither the electric charge nor magnetic charge of black holes is zero. That is to say, the scalarized black hole solution can only appear in cases with nonvanishing electric and magnetic charges. The gravity part of the field equations is not affected by the electromagnetic Chern–Simons term and it only provides an effective potential to the equation of motion for the scalar field. When we pick the coupling constant, electric charge, and magnetic charge appropriately, the dyonic RN black hole will become unstable and there will exist scalarized black hole solutions.

First of all, we investigated the perturbation of the dyonic RN black holes and get the perturbation solutions of the scalar field satisfied the asymptotic flatness condition, which

is just the bifurcation points of dyonic RN solution and scalarized solution in nonlinear cases. Our result shows that the bifurcation points only appear if the parameters satisfy $\zeta = 2Q_e Q_m \lambda^2 > Q_{tot}^2/4$, which also leads to $\lambda^2 > 1/4$. Then, by employing the shooting method, we calculated the scalarized black hole solutions bifurcating from the dyonic RN black hole solution. As a result, there exist some discrete branches of the scalarized solutions and all scalarized branches bifurcate with the GR branch. Different from the dyonic RN black holes, the scalarized dyonic RN black holes can be overcharged (i.e., $M^2 < Q_{tot}^2$) and their mass could even approach zero. This means that the scalarized solution enlarges the range of mass in GR. By analyzing the scalarized configurations with different coupling constant λ and reduced magnetic charge $\tilde{Q}_m$, we can conclude that the stronger interaction can lead to larger scalar hair. Moreover, we studied the entropy and temperature of the scalarized dyonic RN black holes as well. The results show that the entropy for all scalarized black holes exceeds the counterpart of dyonic RN black holes and the first scalarized branch
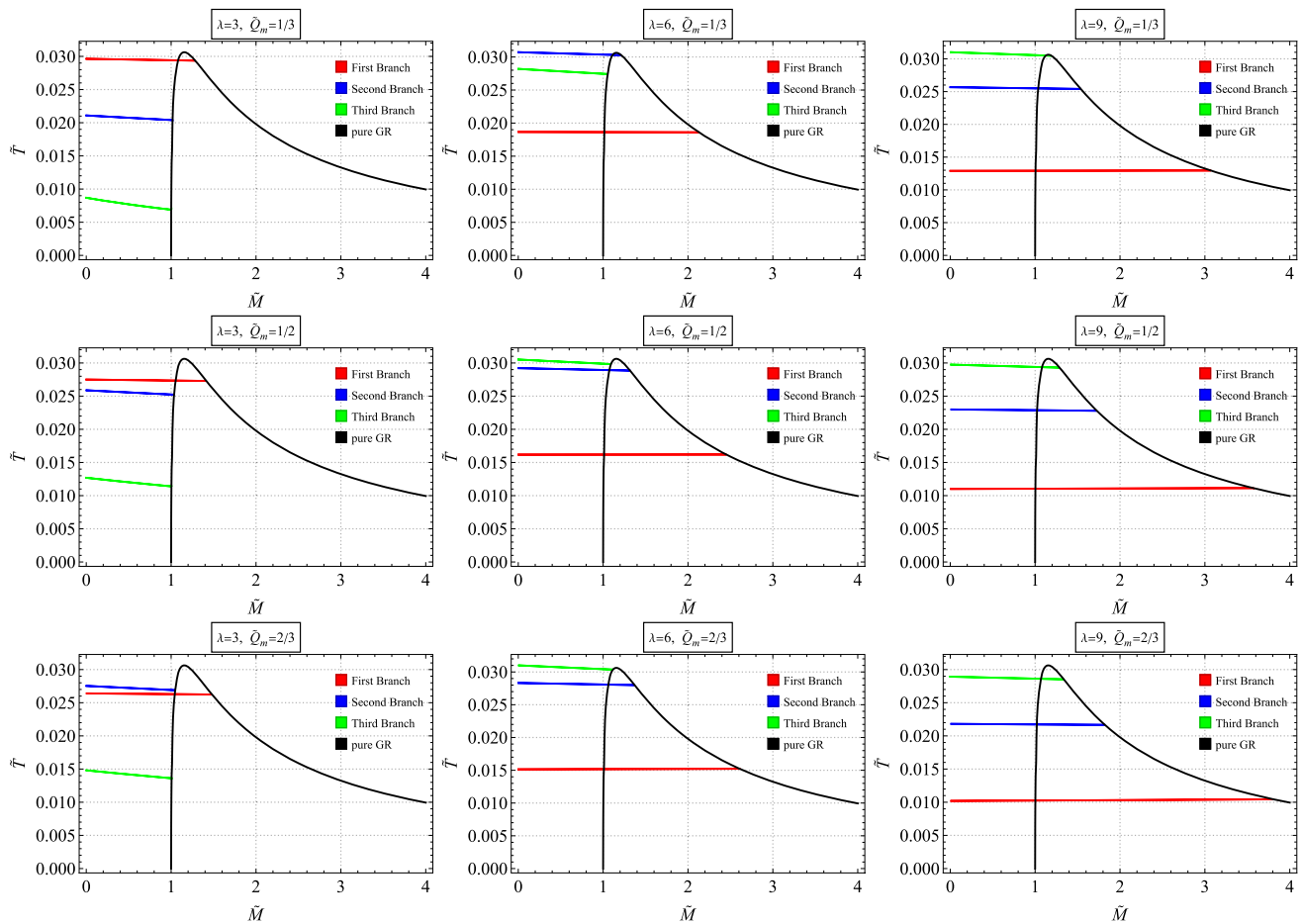
Fig. 8 Plots show the reduced temperature $\tilde{T}$ of black holes as a function of its reduced mass $\tilde{M}$ with different values of the coupling constant λ and reduced magnetic charge $\tilde{Q}_m$ for the first three branches of scalarized dyonic RN black hole

captures the largest entropy, which means that the scalarized configurations might be thermodynamically more stable than GR configurations. By comparing the results of different λ and $\tilde{Q}_m$, we also found that the stronger interaction can make the scalarized configuration has a larger entropy. These imply that the scalarization might be more likely to appear in situations with stronger interaction between the scalar field and the electromagnetic field. From the analysis of black hole temperature, we found that the extremal limit $T = 0$ cannot be reached in the scalarized branches because these branches are ended at the point where the black hole mass vanishes.

In this paper, we only discussed the black hole entropy of the scalarized solutions. However, this does not indicate that the scalarized black holes are dynamically stable. It is also necessary to consider the dynamical stability of these scalarized black holes obtained in this paper and this will be left for our future work. Moreover, it is also interesting to extend the discussion into the dynamical situation to study the scalarization or into the spinning cases to consider the spin-induced scalarization.

References

1. W. Israel, Event horizons in static vacuum space-times. Phys. Rev. **164**, 1776–1779 (1967)

2. B. Carter, Axisymmetric black hole has only two degrees of freedom. Phys. Rev. Lett. **26**, 331–333 (1971)

3. R. Ruffini, J.A. Wheeler, Introducing the black hole. Phys. Today **24**(1), 30 (1971)

4. M.S. Volkov, D.V. Galtsov, Non-Abelian Einstein Yang–Mills black holes. JETP Lett. **50**, 346 (1989)

5. P. Bizon, Colored black holes. Phys. Rev. Lett. **64**, 2844–2847 (1990)

6. B.R. Greene, S.D. Mathur, C.M. O'Neill, Eluding the no hair conjecture: black holes in spontaneously broken gauge theories. Phys. Rev. D **47**, 2242–2259 (1993)

7. P. Kanti, N.E. Mavromatos, J. Rizos, K. Tamvakis, E. Winstanley, Dilatonic black holes in higher curvature string gravity. Phys. Rev. D **54**, 5049–5058 (1996)

8. H. Luckock, I. Moss, Black holes have Skyrmion hair. Phys. Lett. B **176**, 341–345 (1986)

9. S. Droz, M. Heusler, N. Straumann, New black hole solutions with hair. Phys. Lett. B **268**, 371–376 (1991)

10. C.A.R. Herdeiro, E. Radu, Asymptotically flat black holes with scalar hair: a review. Int. J. Mod. Phys. D **24**(09), 1542014 (2015)

11. B.P. Abbott et al., [LIGO Scientific and Virgo], Observation of gravitational waves from a binary black hole merger. Phys. Rev. Lett. **116**(6), 061102 (2016)

12. C.R. Mann, H. Richer, J. Heyl, J. Anderson, J. Kalirai, I. Caiazzo, S. Möhle, A. Knee, H. Baumgardt, A multimass velocity dispersion model of 47 Tucanae indicates no evidence for an intermediate-mass black hole. Astrophys. J. **875**(1), 1 (2019)

13. T. Damour, G. Esposito-Farese, Nonperturbative strong field effects in tensor–scalar theories of gravitation. Phys. Rev. Lett. **70**, 2220–2223 (1993)

14. I.Z. Stefanov, S.S. Yazadjiev, M.D. Todorov, Phases of 4D scalar–tensor black holes coupled to Born–Infeld nonlinear electrodynamics. Mod. Phys. Lett. A **23**, 2915–2931 (2008)

15. D.D. Doneva, S.S. Yazadjiev, K.D. Kokkotas, I.Z. Stefanov, Quasinormal modes, bifurcations and non-uniqueness of charged scalar–tensor black holes. Phys. Rev. D **82**, 064030 (2010)

16. V. Cardoso, I.P. Carucci, P. Pani, T.P. Sotiriou, Matter around Kerr black holes in scalar–tensor theories: scalarization and superradiant instability. Phys. Rev. D **88**, 044056 (2013)

17. V. Cardoso, I.P. Carucci, P. Pani, T.P. Sotiriou, Black holes with surrounding matter in scalar–tensor theories. Phys. Rev. Lett. **111**, 111101 (2013)

18. D.D. Doneva, S.S. Yazadjiev, New Gauss–Bonnet black holes with curvature-induced scalarization in extended scalar–tensor theories. Phys. Rev. Lett. **120**(13), 131103 (2018)

19. H.O. Silva, J. Sakstein, L. Gualtieri, T.P. Sotiriou, E. Berti, Spontaneous scalarization of black holes and compact stars from a Gauss–Bonnet coupling. Phys. Rev. Lett. **120**(13), 131104 (2018)

20. D.D. Doneva, S. Kiorpelidi, P.G. Nedkova, E. Papantonopoulos, S.S. Yazadjiev, Charged Gauss–Bonnet black holes with curvature induced scalarization in the extended scalar–tensor theories. Phys. Rev. D **98**(10), 104056 (2018)

21. G. Antoniou, A. Bakopoulos, P. Kanti, Evasion of No–Hair theorems and novel black-hole solutions in Gauss–Bonnet theories. Phys. Rev. Lett. **120**(13), 131102 (2018)

22. P.V.P. Cunha, C.A.R. Herdeiro, E. Radu, Spontaneously scalarized Kerr black holes in extended scalar–tensor-Gauss–Bonnet gravity. Phys. Rev. Lett. **123**(1), 011101 (2019)

23. C.A.R. Herdeiro, E. Radu, H.O. Silva, T.P. Sotiriou, N. Yunes, Spin-induced scalarized black holes. Phys. Rev. Lett. **126**(1), 011103 (2021)

24. E. Berti, L.G. Collodel, B. Kleihaus, J. Kunz, Spin-induced black-hole scalarization in Einstein-scalar-Gauss–Bonnet theory. Phys. Rev. Lett. **126**(1), 011104 (2021)

25. A. Dima, E. Barausse, N. Franchini, T.P. Sotiriou, Spin-induced black hole spontaneous scalarization. Phys. Rev. Lett. **125**(23), 231101 (2020)

26. S. Hod, Spin-induced black hole spontaneous scalarization: analytic treatment in the large-coupling regime. Phys. Rev. D **105**(2), 024074 (2022)

27. A. Bakopoulos, G. Antoniou, P. Kanti, Novel black-hole solutions in Einstein-scalar-Gauss–Bonnet theories with a cosmological constant. Phys. Rev. D **99**(6), 064003 (2019)

28. J.L. Ripley, F. Pretorius, Dynamics of a $\mathbb{Z}_2$ symmetric EdGB gravity in spherical symmetry. Class. Quantum Gravity **37**(15), 155003 (2020)

29. D.D. Doneva, S.S. Yazadjiev, Dynamics of the nonrotating and rotating black hole scalarization. Phys. Rev. D **103**(6), 064024 (2021)

30. W.E. East, J.L. Ripley, Dynamics of spontaneous black hole scalarization and mergers in Einstein-scalar-Gauss–Bonnet gravity. Phys. Rev. Lett. **127**(10), 101102 (2021)

31. Y.X. Gao, Y. Huang, D.J. Liu, Scalar perturbations on the background of Kerr black holes in the quadratic dynamical Chern–Simons gravity. Phys. Rev. D **99**(4), 044020 (2019)

32. D.D. Doneva, S.S. Yazadjiev, Spontaneously scalarized black holes in dynamical Chern–Simons gravity: dynamics and equilibrium solutions. Phys. Rev. D **103**(8), 083007 (2021)

33. Y.S. Myung, D.C. Zou, Onset of rotating scalarized black holes in Einstein–Chern–Simons-scalar theory. Phys. Lett. B **814**, 136081 (2021)

34. D.C. Zou, Y.S. Myung, Rotating scalarized black holes in scalar couplings to two topological terms. Phys. Lett. B **820**, 136545 (2021)

35. S.J. Zhang, Massive scalar field perturbation on Kerr black holes in dynamical Chern–Simons gravity. Eur. Phys. J. C **81**(5), 441 (2021)

36. C.A.R. Herdeiro, E. Radu, N. Sanchis-Gual, J.A. Font, Spontaneous scalarization of charged black holes. Phys. Rev. Lett. **121**(10), 101102 (2018)

37. P.G.S. Fernandes, C.A.R. Herdeiro, A.M. Pombo, E. Radu, N. Sanchis-Gual, Spontaneous scalarisation of charged black holes: coupling dependence and dynamical features. Class. Quantum Gravity **36**(13), 134002 (2019)

38. P.G.S. Fernandes, C.A.R. Herdeiro, A.M. Pombo, E. Radu, N. Sanchis-Gual, Charged black holes with axionic-type couplings: Classes of solutions and dynamical scalarization. Phys. Rev. D **100**(8), 084045 (2019)

39. J.L. Blázquez-Salcedo, C.A.R. Herdeiro, J. Kunz, A.M. Pombo, E. Radu, Einstein–Maxwell-scalar black holes: the hot, the cold and the bald. Phys. Lett. B **806**, 135493 (2020)

40. Y. Peng, Scalarization of horizonless reflecting stars: neutral scalar fields non-minimally coupled to Maxwell fields. Phys. Lett. B **804**, 135372 (2020)

41. P. Wang, H. Wu, H. Yang, Scalarized Einstein–Born–Infeld black holes. Phys. Rev. D **103**(10), 104012 (2021)

42. Y.S. Myung, D.C. Zou, Scalarized black holes in the Einstein–Maxwell-scalar theory with a quasitopological term. Phys. Rev. D **103**(2), 024010 (2021)

43. D. Astefanesei, C. Herdeiro, J. Oliveira, E. Radu, Higher dimensional black hole scalarization. J. High Energy Phys. **09**, 186 (2020)

44. D. Astefanesei, C. Herdeiro, A. Pombo, E. Radu, Einstein–Maxwell-scalar black holes: classes of solutions, dyons and extremality. J. High Energy Phys. **10**, 078 (2019)

45. Y. Brihaye, C. Herdeiro, E. Radu, Black hole spontaneous scalarisation with a positive cosmological constant. Phys. Lett. B **802**, 135269 (2020)

46. G. Guo, P. Wang, H. Wu, H. Yang, Scalarized Einstein–Maxwell-scalar black holes in anti-de Sitter spacetime. Eur. Phys. J. C **81**(10), 864 (2021)

47. F. Yao, Scalarized Einstein–Maxwell-scalar black holes in a cavity. Eur. Phys. J. C **81**(11), 1009 (2021)

48. S. Mahapatra, S. Priyadarshinee, G.N. Reddy, B. Shukla, Exact topological charged hairy black holes in AdS Space in *D*-dimensions. Phys. Rev. D **102**(2), 024042 (2020)

49. Y.S. Myung, D.C. Zou, Instability of Reissner–Nordström black hole in Einstein–Maxwell-scalar theory. Eur. Phys. J. C **79**(3), 273 (2019)

50. Y.S. Myung, D.C. Zou, Stability of scalarized charged black holes in the Einstein–Maxwell-scalar theory. Eur. Phys. J. C **79**(8), 641 (2019)

51. D.C. Zou, Y.S. Myung, Radial perturbations of the scalarized black holes in Einstein–Maxwell-conformally coupled scalar theory. Phys. Rev. D **102**(6), 064011 (2020)

52. Y.S. Myung, D.C. Zou, Quasinormal modes of scalarized black holes in the Einstein–Maxwell-scalar theory. Phys. Lett. B **790**, 400–407 (2019)

53. J. Luis Blázquez-Salcedo, C.A.R. Herdeiro, S. Kahlen, J. Kunz, A.M. Pombo, E. Radu, Quasinormal modes of hot, cold and bald Einstein–Maxwell-scalar black holes. Eur. Phys. J. C **81**(2), 155 (2021)

54. R.A. Konoplya, A. Zhidenko, Analytical representation for metrics of scalarized Einstein–Maxwell black holes and their shadows. Phys. Rev. D **100**(4), 044015 (2019)

55. S. Hod, Spontaneous scalarization of charged Reissner-Nordström black holes: analytic treatment along the existence line. Phys. Lett. B **798**, 135025 (2019)

56. S. Hod, Reissner–Nordström black holes supporting nonminimally coupled massive scalar field configurations. Phys. Rev. D **101**(10), 104025 (2020)

57. C.Y. Zhang, P. Liu, Y. Liu, C. Niu, B. Wang, Dynamical charged black hole spontaneous scalarization in anti-de Sitter spacetimes. Phys. Rev. D **104**(8), 084089 (2021)

58. C.Y. Zhang, P. Liu, Y. Liu, C. Niu, B. Wang, Dynamical scalarization in Einstein–Maxwell-dilaton theory. Phys. Rev. D **105**(2), 024073 (2022)

59. J.L. Blázquez-Salcedo, S. Kahlen, J. Kunz, Critical solutions of scalarized black holes. Symmetry **12**(12), 2057 (2020)

60. C.Y. Zhang, Q. Chen, Y. Liu, W.K. Luo, Y. Tian, B. Wang, Critical phenomena in dynamical scalarization of charged black holes. Phys. Rev. Lett. **128**(16), 161105 (2022)

61. C.Y. Zhang, Q. Chen, Y. Liu, W.K. Luo, Y. Tian, B. Wang, Dynamical transitions in scalarization and descalarization through black hole accretion. arXiv:2204.09260 [gr-qc]

62. L.F. Abbott, P. Sikivie, A cosmological bound on the invisible axion. Phys. Lett. B **120**, 133–136 (1983)

63. M.A. Fedderke, P.W. Graham, S. Rajendran, Axion dark matter detection with CMB polarization. Phys. Rev. D **100**(1), 015040 (2019)

64. R.T. Co, A. Pierce, Z. Zhang, Y. Zhao, Dark photon dark matter produced by axion oscillations. Phys. Rev. D **99**(7), 075002 (2019)

65. F.P. Huang, K. Kadota, T. Sekiguchi, H. Tashiro, Radio telescope search for the resonant conversion of cold dark matter axions from the magnetized astrophysical sources. Phys. Rev. D **97**(12), 123001 (2018)

66. J.W. Foster, Y. Kahn, O. Macias, Z. Sun, R.P. Eatough, V.I. Kondratiev, W.M. Peters, C. Weniger, B.R. Safdi, Green Bank and Effelsberg radio telescope searches for axion dark matter conversion in neutron star magnetospheres. Phys. Rev. Lett. **125**(17), 171301 (2020)

67. J.G. Rosa, T.W. Kephart, Stimulated axion decay in superradiant clouds around primordial black holes. Phys. Rev. Lett. **120**(23), 231102 (2018)

68. W. Buell, B. Shadwick, Potentials and bound states. Am. J. Phys. **63**, 256 (1995)

69. R.A. Konoplya, A. Zhidenko, Quasinormal modes of black holes: from astrophysics to string theory. Rev. Mod. Phys. **83**, 793–836 (2011)